INSTITUTE OF PHYSICS PUBLISHING NONLINEARITY

Nonlinearity **18** (2005) 2565–2580 doi:10.1088/0951-7715/18/6/008

Critical points of the Onsager functional on a sphere

I Fatkullin[1] **and V Slastikov**[2,3]

[1] Department of Mathematics, University of Arizona, Tucson, AZ, USA
[2] Center for Nonlinear Analysis, Department of Mathematical Sciences, Carnegie Mellon University, Pittsburgh, PA, USA

E-mail: ibrahim@math.arizona.edu and slastiko@andrew.cmu.edu

Received 13 January 2005, in final form 8 August 2005
Published 31 August 2005
Online at stacks.iop.org/Non/18/2565

Recommended by E S Titi

Abstract

We study Onsager's model of isotropic–nematic phase transitions with orientation parameter on a sphere. We consider two interaction potentials: the antisymmetric (with respect to orientation inversion) dipolar potential and symmetric Maier–Saupe potential. We prove the axial symmetry and derive explicit formulae for all critical points, thus obtaining their complete classification. Finally, we investigate their stability and construct the corresponding bifurcation diagrams.

Mathematics Subject Classification: 82B27, 82D60

Introduction

The theory of isotropic–nematic phase transitions in rod-like polymers and liquid crystals acquired a solid mathematical background when Onsager introduced a variational model relating their equilibrium states to critical points of a *free energy functional* [20]. Ever since, his approach has become the standard way of describing many associated phenomena, both static and dynamic [6, 8, 13]. However, the problem of rigorous analysis and classification of all critical points of Onsager's functional remained open, and only recently has significant progress beyond numerical and approximate results been achieved.

Let us begin by reviewing the major contributions to the theory. Onsager's original approach is based on the second virial approximation: the second virial coefficient was calculated for excluded volume interaction between the rods which results in the $|\boldsymbol{x} \times \boldsymbol{x}'|$ potential in the variational model ($\boldsymbol{x}$ stands for the *director* of the rod). Due to the non-analytic nature of this potential no exact non-trivial solutions can be obtained, and Onsager used a variational approximation in his studies. The work by Maier and Saupe [19] suggested that using a similar but analytic potential $-(\boldsymbol{x}\cdot\boldsymbol{x}')^2 + 1/3$ would yield quantitatively correct results;

[3] Present address: Warwick Mathematics Institute, the University of Warwick, Coventry, UK.

however their investigations involved an additional approximation of the *uniaxial mean-field*. (Most of the subsequent studies, as well as ours, employ the Maier–Saupe potential rather than the original Onsager potential.) A paper by Freiser [11] extends the Maier–Saupe interaction for applicability to the systems with asymmetrical molecules. Kayser and Raveché [14] developed an iterative scheme for computation of the axially-symmetric critical points of the original Onsager model. A mean-field approximation producing equations similar to those of the Maier–Saupe theory was made by Doi [7], who analysed bifurcations which occur as the mean field is varied. Some of the first numerical solutions were obtained by Larson and Ottinger [17] (see also references within) who studied the gradient flow equations for the Onsager functional (usually referred to as Doi, or Smoluchowski, equations). Effects of the steady state shear and elongational flows on the Doi bifurcation diagram were numerically investigated by Bhave *et al* [2]. These studies were then extended by Wang [21]; Bhandar and Wiest [1], who considered additional factors, e.g. an external mean-field magnetic potential. The highly resolved numerical simulations by Forest *et al* (see, e.g. [10]) reveal many fine details that appear once various small perturbations are applied to the system. Additional references to various numerical results in related models may be found in the review by Kröger [16].

On the rigorous analytical side the current results include a detailed study of a reduced model (rod orientation is assumed to lie on a circle) by Constantin *et al* [4] and Constantin and Vukadinovic [5], Luo *et al* [18] and the authors [9]. Constantin *et al* also considered the full model on a sphere [3] and deduced an upper bound on the number of critical points from the analysis of a transcendental equation (*constitutive equation*) for the orientational order tensor. However the principal difficulty hindering a complete classification of all critical points, i.e. a rigorous proof of their axial symmetry, still had not been addressed.

In this work we prove the axial symmetry of all critical points of the Onsager functional on a sphere with dipolar and Maier–Saupe interaction potentials. We also extend the methods employed in [9] for the model on a circle and derive explicit analytical expressions for all critical points and investigate their stability and bifurcations. (Note that we do not make any additional approximations beyond Onsager's second virial approximation.) As a result we produce a complete analytical solution to this remarkable model in statistical physics of polymers.

Let us review the model and outline our most important results. The state of the system (a liquid–crystalline suspension) is described by a probability density of rod orientations $\rho(s)$. The orientation parameter s belongs to a unit sphere $\mathbb{S}^2$ in a three-dimensional Euclidean space. Throughout this paper we routinely use alternative notations for the points on the unit sphere, e.g. $s \in \mathbb{S}^2$ may be represented as a unit vector in Cartesian coordinates: $\boldsymbol{x} = (x_1, x_2, x_3) \in \mathbb{R}^3$, $|\boldsymbol{x}| = 1$; or as angles, $\varphi \in [0, 2\pi)$, $\theta \in [0, \pi]$ in a spherical coordinate frame. In the last case, unless the polar axis ($\theta = 0$) and the plane $\varphi = 0$ are prescribed explicitly, they may be chosen arbitrarily.

The Onsager free energy functional may be written as

$$\mathcal{F}[\rho] := \int_{\mathbb{S}^2} \left[\tau \rho(s) \ln \rho(s) + \frac{1}{2} \rho(s) \int_{\mathbb{S}^2} U(s, s') \rho(s') \, \mathrm{d}s' \right] \mathrm{d}s. \tag{1}$$

The first term under the integral is the *entropic term*, the positive parameter τ is the *temperature* (the Boltzmann's constant is set to unity). This term is minimized by the uniform density $\bar{\rho}(s) \equiv 1/4\pi$ and is dominant when τ is large. The second term is the *interaction term*, the function $U(s, s')$ is called *interaction potential* (it corresponds to the second virial coefficient). In this work we consider two interaction potentials: the *dipolar potential*

$$U_{\mathrm{d}}(\boldsymbol{x}, \boldsymbol{x}') := -\boldsymbol{x} \cdot \boldsymbol{x}' \tag{2}$$

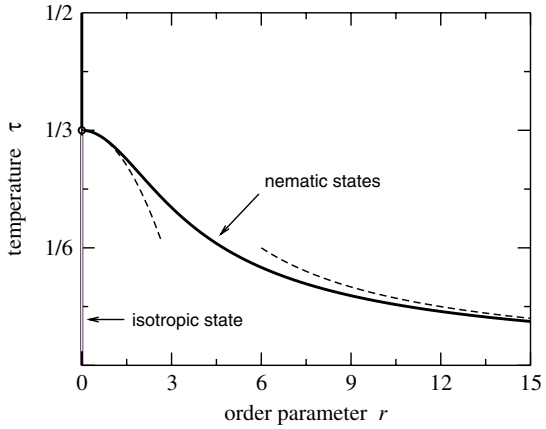

Figure 1. Isotropic–nematic phase diagram for the dipolar interaction. The bell-shaped curve (symmetric about zero) is the graph of the temperature τ versus the order parameter r, given by (20). The thick solid line corresponds to the stable branches: the trivial state, $\Phi \equiv 0$, for $\tau > 1/3$; and the family (19) for $\tau < 1/3$. The hollow line marks the unstable state, $\Phi \equiv 0$, when $\tau < 1/3$; the dashed lines represent asymptotic expansions (25).

and the *Maier–Saupe potential* [19]

$$U_{\mathrm{ms}}(\boldsymbol{x}, \boldsymbol{x}') := -(\boldsymbol{x} \cdot \boldsymbol{x}')^2 + \tfrac{1}{3}. \tag{3}$$

The principal difference between these two potentials is that the Maier–Saupe potential remains invariant when one of its arguments changes sign; thus it is indifferent to inversion of the rod orientations. The dipolar potential, in contrast, prefers that all rods have the same orientation; in a sense, such an interaction may be considered an interaction of 'arrows' rather than 'rods'. Physically this corresponds to the situation when the polymer molecules possess dipole moment.

In our paper we fix the strength of interaction and vary the temperature τ. Note that since the system is *athermal* [6, 13], it may seem more appropriate to fix τ and vary the interaction strength (concentration of polymer molecules in the fluid). However, choosing τ as a parameter simplifies many calculations; moreover it only makes a semantical difference: the interaction strength corresponds (mathematically) to the inverse temperature.

It is not hard to see that the uniform density $\bar{\rho} \equiv 1/4\pi$ is a critical point of the free energy functional (1) for any τ. It describes the disordered, isotropic phase. For the dipolar potential we prove that $\bar{\rho}$ is a unique critical point (and the global minimizer) when $\tau \geqslant \tau_c := 1/3$. At $\tau = \tau_c$ it loses stability as a result of a pitchfork bifurcation, and a family of critical points given by (in a suitable spherical coordinate frame)

$$\rho_{\mathrm{d}}(\varphi, \theta) := \mathcal{Z}^{-1}\, \mathrm{e}^{-r(\tau)\cos\theta} \tag{4}$$

appears. The *order parameter* $r(\tau)$ is obtained inverting (20). These states become the global (non-isolated) minimizers and describe the ordered, nematic phase. No other critical points exist. The corresponding bifurcation diagram (*isotropic–nematic phase diagram*) is displayed in figure 1.

For the Maier–Saupe potential we prove that the uniform density is a unique critical point when $\tau > \tau^* \approx 0.149$ and an isolated minimizer for $\tau > \tau_c = 2/15$. At $\tau = \tau^*$ a saddle-node bifurcation (a fold) occurs (away from the uniform state), and *two* families of critical points

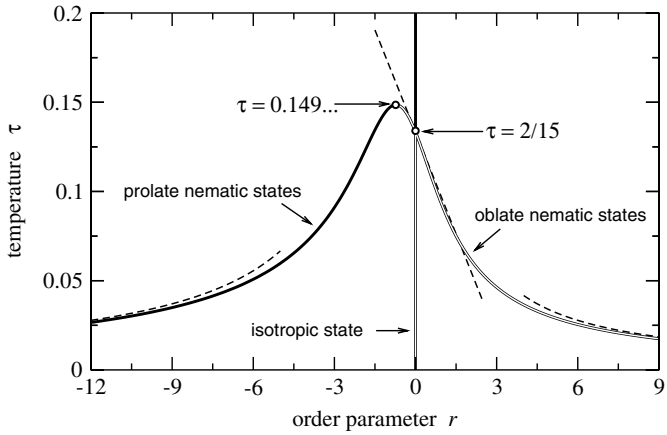

Figure 2. Isotropic–nematic phase diagram for the Maier–Saupe interaction. The bell-shaped curve is the graph of the temperature τ versus the order parameter r, given by (27). The thick solid line corresponds to the stable branches: the trivial state, $\Phi \equiv 0$, for $\tau > 2/15$; and the stable prolate family for $\tau < \tau^*$. The hollow line marks the unstable states, the dashed lines represent asymptotic expansions (37).

given by (in a suitable spherical coordinate frame)

$$\rho_{\mathrm{ms}}(\varphi, \theta) := \mathcal{Z}^{-1}\, \mathrm{e}^{-r_{1,2}(\tau)(3\cos^2\theta - 1)} \tag{5}$$

emerge; the functions $r_{1,2}(\tau)$ are obtained inverting (27). No other critical points exist. When $\tau \in (\tau_c, \tau^*)$ both families correspond to *prolate* nematic states; respective probability densities are concentrated near the poles of the sphere. One of these families is stable, the other is unstable. The stable prolate states persist for $\tau \in (0, \tau_c)$ and become global (non-isolated) minimizers at some $\tau_* \in (\tau_c, \tau^*)$. At $\tau = \tau_c$ the unstable prolate states 'collide' with the uniform state and a transcritical bifurcation occurs. As a result, the uniform state loses stability, and the unstable prolate states become unstable *oblate* states (respective probability densities are concentrated near the big circles of the sphere). These unstable oblate states persist for all $\tau \in (0, \tau_c)$. The isotropic–nematic phase diagram for the Maier–Saupe potential is presented in figure 2 (observe its similarity to the Doi's mean-field phase diagram [7]).

1. Some properties of interaction potentials and critical points

Let us first discuss a few simple but important properties of interaction potentials and critical points of the free energy functional. Some properties of spherical harmonics are summarized in appendix B.

Representations of interaction potentials. Observe that potentials (2) and (3) are eigenfunctions of the Laplace–Beltrami operator (B4) on $\mathbb{S}^2$:

$$\Delta U(s, s') = \lambda U(s, s'), \tag{6}$$

Δ may act on either variable. For the dipolar interaction $\lambda = -2$, and for the Maier–Saupe potential $\lambda = -6$. The corresponding eigenspaces Λ_1 and Λ_2 are three- and five-dimensional and are spanned by spherical harmonics $y_{l,m}(s)$ of the first and second-order respectively ($l = 1, 2$, $m = -l, \ldots, l$). Therefore, we may expand $U(s, s')$ in the corresponding bases:

using (B7) we get

$$U_{\mathrm{d}}(s,s') = -P_1(\boldsymbol{e}\cdot\boldsymbol{e}') = u_{\mathrm{d}}\sum_{m=-1}^{1} y_{1,m}(s)\,y^*_{1,m}(s'), \qquad u_{\mathrm{d}} := -\frac{4\pi}{3};$$
$$U_{\mathrm{ms}}(s,s') = -\frac{2}{3}P_2(\boldsymbol{e}\cdot\boldsymbol{e}') = u_{\mathrm{ms}}\sum_{m=-2}^{2} y_{2,m}(s)y^*_{2,m}(s'), \qquad u_{\mathrm{ms}} := -\frac{8\pi}{15}. \tag{7}$$

Euler–Lagrange equation. Let us introduce the *thermodynamic potential* $\Phi(s)$ setting

$$\rho(s) =: \mathcal{Z}^{-1}\mathrm{e}^{-\Phi(s)}, \qquad \mathcal{Z} = \int_{\mathbb{S}^2}\mathrm{e}^{-\Phi(s)}\,\mathrm{d}s. \tag{8}$$

The normalizing constant $\mathcal{Z}$ is called the *partition integral.* Note that $\Phi(s)$ is defined up to an additive constant which is chosen so that $\Phi(s)$ integrates to zero over the sphere. The Euler–Lagrange equation for critical points of the free energy functional (1) may now be written as

$$\tau\Phi(s) = \int_{\mathbb{S}^2} U(s,s')\rho(s')\,\mathrm{d}s'. \tag{9}$$

In this paper we mainly deal with the thermodynamic potential $\Phi(s)$, and the properties of the corresponding probability density $\rho(s)$ may be reconstructed from (8).

Applying the Laplace–Beltrami operator on both sides of (9) and using (6) we obtain

$$\Delta\Phi(s) = \lambda\Phi(s), \tag{10}$$

i.e. $\Phi(s)$ is an eigenfunction corresponding to the same eigenvalue as $U(s,s')$. This implies that it may be expanded on the same basis $\{y_{l,m}(s)\}$:

$$\Phi(s) = \sum_{m=-l}^{l}\phi_m y_{l,m}(s). \tag{11}$$

We may regard the partition integral $\mathcal{Z}$ as a function of the coefficients ϕ_m satisfying $\phi^*_m = \phi_{-m}$ (this condition is assumed from now on, as we are interested in real solutions):

$$\mathcal{Z}(\phi) = \int_{\mathbb{S}^2}\mathrm{e}^{-\sum_m \phi_m y_{l,m}(s)}\,\mathrm{d}s. \tag{12}$$

Hereafter summation over m is always taken over the whole range $-l,\dots,l$. Rewriting the Euler–Lagrange equation in Fourier coordinates (for the coefficients ϕ_m) we obtain

$$\tau\phi_m = u\mathcal{Z}^{-1}\int_{\mathbb{S}^2} y^*_{l,m}(s)\,\mathrm{e}^{-\sum_{m'}\phi_{m'}\,y_{l,m'}(s)}\,\mathrm{d}s \tag{13}$$

and the constant u is defined in (7). Note that $y^*_{l,m}(s) = y_{l,-m}(s)$. Equation (13) are equivalent to the original Euler–Lagrange equation (9): an arbitrary set of the coefficients, ϕ_m, produces a solution of (9) if and only if for any m,

$$\tau = -\frac{u}{\phi_m}\frac{\partial}{\partial\phi^*_m}\ln\mathcal{Z}(\phi). \tag{14}$$

If $\phi_m = 0$ for some m, we have to verify directly that respective integral in (13) produces zero. Finally, let us note that the free energy of a critical point may be found (using the Euler–Lagrange equation) as

$$\mathcal{F}[\rho] = -\frac{\tau^2}{2u}\|\Phi\|^2 - \tau\ln\mathcal{Z}. \tag{15}$$

Now let us consider individually the cases with dipolar and Maier–Saupe interaction potentials in greater detail.

2. Critical points for the dipolar interaction potential

For the dipolar potential $U(\boldsymbol{x}, \boldsymbol{x}') = -\boldsymbol{x} \cdot \boldsymbol{x}'$ we may compute the partition integral (for any values of the parameters ϕ_m) explicitly. Rewriting (12) in spherical coordinates (using (B6), $l = 1$) we get

$$\mathcal{Z}(\phi) = \int_0^{\pi} \int_0^{2\pi} \mathrm{e}^{\alpha \cos\theta + (\beta \cos\varphi + \gamma \sin\varphi)\sin\theta} \sin\theta \, \mathrm{d}\varphi \, \mathrm{d}\theta. \tag{16}$$

The parameters, α, β and γ, may be easily related to the coefficients ϕ_m; however it is sufficient to observe that

$$r^2 := \alpha^2 + \beta^2 + \gamma^2 = \frac{3}{4\pi}|\phi|^2. \tag{17}$$

Integral (16) becomes elementary after an appropriate rotation in $\mathbb{R}^3$ (see, e.g. [12]):

$$\mathcal{Z}(\phi) = \int_0^{2\pi} \int_0^{\pi} \mathrm{e}^{r\cos\theta} \sin\theta \, \mathrm{d}\varphi \, \mathrm{d}\theta = 4\pi \frac{1}{r} \sinh r. \tag{18}$$

From the Euler–Lagrange equation (9) we may immediately deduce that for all temperatures τ there exists a trivial solution, $\Phi \equiv 0$ (corresponding to $r = 0$, $\mathcal{Z} = 4\pi$). All other critical points may be classified by means of the following theorem.

Theorem 1. *A function $\Phi(s)$ is a nontrivial solution of the Euler–Lagrange equation (9) with dipolar interaction potential if and only if it may be represented as*

$$\Phi(\varphi, \theta) = r \cos\theta, \qquad r > 0 \tag{19}$$

in some spherical coordinate frame. The order parameter r and the temperature τ are related by

$$\tau = \frac{1}{r^2}(r \coth r - 1). \tag{20}$$

Remark A. Freedom in the choice of a spherical coordinate frame reflects that a whole family of equivalent solutions may be obtained by an arbitrary rotation of a given solution.

Remark B. Equation (20) is solvable for r if and only if, $0 < \tau \leqslant 1/3$. It has two solutions which differ by sign; however it is sufficient to consider $r > 0$: the transformation $r \mapsto -r$ corresponds to inversion of the polar axis and does not produce new critical points.

Proof. As shown in section 1, all solutions of (9) belong to the subspace Λ_1 spanned by the first-order spherical harmonics $y_{1,m}(s)$. Therefore, after a suitable rotation, any solution may be represented as (19). Equivalently, this may be obtained observing that (9) implies (in Cartesian coordinates)

$$\tau \Phi(\boldsymbol{x}) = \boldsymbol{x} \cdot \boldsymbol{e}, \qquad \boldsymbol{e} := -\int_{|\boldsymbol{y}|=1} \boldsymbol{x} \rho(\boldsymbol{x}) \, \mathrm{d}s(\boldsymbol{x}). \tag{21}$$

Choosing $\boldsymbol{e}$ as the polar axis for a spherical coordinate frame, we obtain (19). Note that all solutions are axially-symmetric (independent of the latitudinal angle φ in an appropriate spherical coordinate frame).

Now let us verify that any function of the form (19) satisfies the Euler–Lagrange equation and obtain a relation between r and the temperature τ. From the explicit formulae for spherical harmonics (B6) we conclude that

$$\phi_0 = \left[\frac{4\pi}{3}\right]^{1/2} r, \qquad \phi_{\pm 1} = 0. \tag{22}$$

Using this in (13) we may see that equations for $m \neq 0$ are satisfied trivially (integrals over the latitudinal angle φ produce zeros). Equation for $m = 0$, e.g. in the form (14), provides the value of the temperature τ (recollect $u = -4\pi/3$):

$$\tau = \frac{1}{r}\frac{\mathrm{d}}{\mathrm{d}r}\ln \mathcal{Z}(r). \tag{23}$$

Substituting an explicit expression for the partition integral (18), we obtain (20). □

2.1. Stability and bifurcation of critical points

A straightforward analysis shows that $\tau(r)$ given by (20) is a positive symmetric bell-like function with the maximum $\tau_c := \tau(0) = 1/3$, as displayed in figure 1. Its range is $(0, 1/3]$; thus equation (20) has a unique positive solution r for any $\tau \in (0, 1/3)$. We conclude that for $\tau > \tau_c$ the only critical point is the trivial solution $\Phi \equiv 0$, whereas for $\tau < \tau_c$ there also exists a family of rotation-equivalent solutions described by theorem 1.

Let us analyse the stability of critical points. Consider the trivial solution $\Phi \equiv 0$ and the corresponding probability density $\bar{\rho} \equiv 1/4\pi$. The second variation of the free energy functional (1) may be written (expanding in terms of spherical harmonics) as

$$\mathbf{D}^2\mathcal{F}_{|\bar{\rho}}[\eta] = 4\pi\tau \sum_{l=0}^{\infty}\sum_{m=-l}^{l} |\eta_{l,m}|^2 - \frac{4\pi}{3}\sum_{m=-1}^{1} |\eta_{1,m}|^2. \tag{24}$$

Here η is the variation of the probability density $\bar{\rho}$. We see that the second variation is positive for any η if and only if $\tau > 1/3 = \tau_c$. Consequently, the trivial solution is the global (isolated) minimizer for $\tau > \tau_c$. At $\tau = \tau_c$ a pitchfork bifurcation occurs, and stability is transferred to the family of nontrivial solutions, which become global (non-isolated) minimizers. The same result may be obtained by direct comparison of the free energies of respective critical points using formula (15). Summarizing all of the above, we obtain the following theorem.

Theorem 2. *When $\tau \geqslant \tau_c = 1/3$ the only critical point of the free energy functional (1) with dipolar interaction potential is the uniform density $\bar{\rho} \equiv 1/4\pi$, which is the global minimizer. When $\tau < \tau_c$ this (trivial) state becomes unstable and there exists exactly one family of rotation-equivalent non-trivial critical points, described by theorem 1, which are the global (non-isolated) minimizers.*

For completeness, let us also present the leading-order asymptotic expansions of the order parameter r as a function of τ; they may be easily derived from (20). The corresponding graphs are displayed in figure 1.

$$\begin{aligned} r &= \frac{1}{\tau} + \mathcal{O}(1), \qquad && \tau \downarrow 0; \\ r^2 &= 45(\tau_c - \tau) + \mathcal{O}(\tau_c - \tau)^2, \qquad && \tau \uparrow \tau_c. \end{aligned} \tag{25}$$

3. Critical points for the Maier–Saupe interaction potential

Now we consider the Maier–Saupe interaction potential $U(\boldsymbol{x}, \boldsymbol{x}') = -(\boldsymbol{x}\cdot\boldsymbol{x}')^2 + 1/3$. Although it is possible to compute the partition integral (for an arbitrary set of parameters ϕ_m) in terms of hypergeometric series, such a representation does not allow us to extract much of the required information, and we have to resort to a more delicate analysis.

As in the case of dipolar interaction, there exists a trivial solution $\Phi \equiv 0$, valid for all temperatures τ. All other solutions may be classified using the following theorem.

Theorem 3. *A function $\Phi(s)$ is a non-trivial solution of the Euler–Lagrange equation (9) with Maier–Saupe interaction potential if and only if it may be represented as*

$$\Phi(\varphi,\theta) = r(3\cos^2\theta - 1), \qquad r \neq 0 \tag{26}$$

in some spherical coordinate frame. The order parameter r and the temperature τ are related by

$$\tau = \frac{1}{6r}\left[1 - \frac{1}{2r} + \left[\frac{3}{\pi r}\right]^{1/2} \frac{\mathrm{e}^{-3r}}{\operatorname{erf}\sqrt{3r}}\right]. \tag{27}$$

Remark A. As in the case of dipolar interaction, a whole family of equivalent critical points may be obtained by an arbitrary rotation of a given solution.

Remark B. Equation (27) is solvable for r if and only if $0 < \tau \leqslant \tau^*$, where τ^* is the unique extremum (maximum) of $\tau(r)$—see discussion following the proof. For any $\tau \in (0, \tau^*)$ there exist exactly two solutions $r_{1,2}(\tau)$ which, unlike in the case of dipolar interaction, produce non-equivalent critical points.

Remark C. From (26) we may see that $\Phi(\varphi,\theta)$ does not depend on the latitudinal angle φ. This immediately implies the axial symmetry of all critical points.

Remark D. When $r < 0$ the probability density $\rho(s) = \mathcal{Z}^{-1}\exp\{-\Phi(s)\}$ is concentrated near the poles of the sphere; such states are called *prolate*. When $r > 0$, $\rho(s)$ is concentrated on a big circle (equator); these states are called *oblate*.

The proof of this theorem is less trivial than in the case of dipolar interaction. We proceed in two steps: first, by direct computation (analogous to the dipolar case) we prove that any axially-symmetric function from Λ_2 (a subspace spanned by second-order spherical harmonics) is a solution, and this accounts for all axially-symmetric solutions. Second, we prove that no other solutions exist. The second part of the proof relies on lemma 1 which is stated and proved in appendix A.

Proof. Let us first find all axially-symmetric solutions. As shown in section 1, the thermodynamic potential $\Phi(s)$ belongs to the subspace Λ_2, spanned by second-order spherical harmonics. Using lemma 3 (appendix B) we conclude that any axially-symmetric solution may be represented in the form (26).

Now let us show that a function in the form (26) solves the Euler–Lagrange equation and obtain the corresponding temperature. From the explicit formulae for spherical harmonics (B6) we find

$$\phi_0 = \left[\frac{16\pi}{5}\right]^{1/2} r, \qquad \phi_{\pm1} = \phi_{\pm2} = 0. \tag{28}$$

Substituting into (13), we may verify that all equations with $m \neq 0$ are trivially satisfied (integrals over the latitudinal angle φ, again, produce zeros). The equation for $m = 0$ provides an expression for the temperature τ. Indeed, computing the partition integral (for this particular combination of ϕ_m, we may express it via elementary functions) we get

$$\mathcal{Z} = \int_0^{\pi}\int_0^{2\pi} \mathrm{e}^{r(1-3\cos^2\theta)}\sin\theta\,\mathrm{d}\varphi\,\mathrm{d}\theta = 2\pi^{3/2}\frac{\mathrm{e}^r}{\sqrt{3r}}\operatorname{erf}\sqrt{3r}. \tag{29}$$

From (14) ($u = -8\pi/15$) we obtain

$$\tau = \frac{1}{6r}\frac{\mathrm{d}}{\mathrm{d}r}\ln\mathcal{Z}(r). \tag{30}$$

An explicit calculation produces (27).

This concludes the first part of the proof: we showed that any axially-symmetric function from Λ_2 satisfies the Euler–Lagrange equation, and establishes a relation between r and the temperature τ, i.e. we have accounted for all axially-symmetric solutions. Now we will prove that there exist no other solutions.

Let us employ a different representation of solutions such as was used in [3]. In Cartesian coordinates the Euler–Lagrange equation (9) may be written as

$$\tau\Phi(\boldsymbol{x}) = -\sum_{i,j=1}^{3} R_{ij}x_i x_j + \frac{1}{3}, \qquad R_{ij} := \int_{|\boldsymbol{x}|=1} x_i x_j \rho(\boldsymbol{x})\,\mathrm{d}s(\boldsymbol{x}). \tag{31}$$

The matrix R_{ij} is symmetric and may be diagonalized by an appropriate rotation. Let us convert to the corresponding coordinate frame. In this case the thermodynamic potential may be represented as

$$\Phi(\boldsymbol{x}) = -\frac{1}{\tau}\left[\lambda_1 x_1^2 + \lambda_2 x_2^2 + \lambda_3 x_3^2 - \frac{1}{3}\right]. \tag{32}$$

We may rewrite the Euler–Lagrange equation as equations for the eigenvalues $\{\lambda_i\}$:

$$\lambda_i = \frac{1}{\mathcal{Z}}\int_{|\boldsymbol{x}|=1} x_i^2 \exp\left\{\frac{1}{\tau}\sum_{j=1}^{3}\lambda_j x_j^2\right\}\mathrm{d}s(\boldsymbol{x}), \qquad \mathcal{Z} := \int_{|\boldsymbol{x}|=1}\exp\left\{\frac{1}{\tau}\sum_{i=1}^{3}\lambda_i x_i^2\right\}\mathrm{d}s(\boldsymbol{x}). \tag{33}$$

Solutions to this equation are in one-to-one correspondence (up to rotation in $\mathbb{R}^3$) with solutions of the original equation (9) (see [3] for a complete proof). From (33) it is easy to see that any solution necessarily satisfies $0 < \lambda_1, \lambda_2, \lambda_3 < 1$, $\lambda_1 + \lambda_2 + \lambda_3 = 1$. However, there exists a more subtle property which is proved in lemma 1 (appendix A): equation (33) is only solvable if $\lambda_i = \lambda_j$ for some $i \neq j$. Assuming (without loss of generality) that $\lambda_1 = \lambda_2$, we may observe that the thermodynamic potential (32) is invariant with respect to rotations around the x_3 axis, i.e. it is axially-symmetric. □

3.1. Stability and bifurcations of critical points

Stability analysis for the model with Maier–Saupe interaction potential is straightforward but quite cumbersome. The reason is that here (unlike in the dipolar case) at low temperatures there exist three families of critical points (see below), and thus we cannot simply compare their free energies to deduce their stability. In what follows we will omit all technical calculations.

Let us first describe a function $\tau(r)$ given by (27). A straightforward calculation shows that this function is positive and has a unique extremum (maximum) $\tau^* := \tau(r^*)$. The values of τ^* and r^* may be obtained by solving the transcendental equation $\tau'(r) = 0$ and seem to have no representation in quadratures. The approximate numerical values are: $r^* \approx -0.726$, $\tau^* \approx 0.149$. The graph of $\tau(r)$ is displayed in figure 2.

We conclude that when $\tau > \tau^*$ the trivial state $\Phi \equiv 0$ is the only critical point of the free energy functional (1), whereas when $\tau < \tau^*$ there exist two more families of rotation-equivalent critical points corresponding to the two branches of the inverse function $r(\tau)$. Let us use the subscript indices '1' and '2' to distinguish between these branches, setting $r_1(\tau) \leqslant r_2(\tau)$ (equality is achieved only when $\tau = \tau^*$). Observe that $r_1(\tau) < 0$, whereas $r_2(\tau) < 0$ for $\tau > 2/15 =: \tau_c$; and $r_2(\tau) > 0$ for $\tau < 2/15$. An important difference from the dipolar case is that the critical points $\Phi_1(s)$ and $\Phi_2(s)$, corresponding to the branches r_1 and r_2 are not equivalent, i.e. may not be matched by rotations. $\Phi_1(s)$ is always a prolate state, whereas $\Phi_2(s)$ is a prolate state for $\tau > \tau_c$ and an oblate state for $\tau < \tau_c$.

Now let us study the stability of the critical points. Consider the trivial solution $\Phi \equiv 0$ and the corresponding probability density $\bar{\rho} \equiv 1/4\pi$. Expanding in terms of spherical harmonics we may write the second variation (Hessian) of the free energy functional (1) as

$$\mathbf{D}^2\mathcal{F}_{|\bar{\rho}}[\eta] = 4\pi\tau \sum_{l=0}^{\infty} \sum_{m=-l}^{l} |\eta_{l,m}|^2 - \frac{8\pi}{15} \sum_{m=-2}^{2} |\eta_{2,m}|^2. \tag{34}$$

Here η is the variation of the probability density $\bar{\rho}$. We see that it is positive for any η if and only if $\tau > 2/15 = \tau_c$. Thus the trivial solution is an isolated minimizer for $\tau > \tau_c$.

Stability analysis for the other branches $\rho_{1,2}(s)$ may be carried out in a similar manner. However, estimating variations of the entropic term near nontrivial solutions is rather tedious. A different approach utilizes the following property.

Proposition 1. *Consider a τ-dependent family of rotation-equivalent critical points of the functional (1). Stability of this family may not change (when τ is varied) while it remains isolated, i.e. no other critical points exist in its sufficiently small neighbourhood.*

Remark. This statement implies that a stable solution branch may only lose stability if some other branch bifurcates from it (or a fold occurs). Since we know all possible solution branches and thus all bifurcation points, we may deduce the stability of any branch by analysing its arbitrary point. We do not provide a detailed proof here. Let us only comment that this proposition is a direct consequence of Krasnosel'skii's theorems for bifurcation points of nonlinear integral operators [15] (see [22] for refinements in the case of potential operators).

A straightforward computation using formula (15) shows that

$$\mathcal{F}[\rho_1] < \mathcal{F}[\rho_2]; \quad \mathcal{F}[\rho_2] < \mathcal{F}[\bar{\rho}] \qquad \text{if and only if } \tau < \tau_c. \tag{35}$$

Thus the critical points corresponding to $r_1(\tau)$ are the global minimizers when $\tau < \tau_c$; in fact, this happens at some $\tau_* \approx 0.148 \in (\tau_c, \tau^*)$. Employing proposition 1 we conclude that the whole branch is stable for $\tau \in (0, \tau^*)$. At $\tau = \tau^*$ the two prolate branches merge and the corresponding state is unstable: its energy is greater than that of the trivial solution (since at this temperature there exist only two nonequivalent critical states this is sufficient to conclude instability). We may classify the bifurcation at $\tau = \tau^*$ as a saddle-node (or a fold) bifurcation.

Similarly we may show that the whole branch $r_2(\tau)$ is unstable for all $\tau \in (0, \tau^*)$. For that we only need to present variations η of the probability density $\rho(s)$, which yield negative values for the Hessian of the free energy functional. By straightforward calculation we may show that when $|r|$ is sufficiently small ($r \neq 0$),

$$\mathbf{D}^2\mathcal{F}_{|\rho_2}[3\cos^2\theta - 1] < 0 \quad \text{for } r < 0; \qquad \mathbf{D}^2\mathcal{F}_{|\rho_2}[\sin^2\theta \cos 2\varphi] < 0 \quad \text{for } r > 0. \tag{36}$$

The first variation, $\eta = 3\cos^2\theta - 1$, stretches the prolate state even more in the direction of the polar axis. It is a variation towards the stable prolate (r_1) state. The second variation, $\eta = \sin^2\theta \cos 2\varphi$, stretches the oblate state in the direction of some axis which crosses the corresponding big circle. It is also a variation towards a stable prolate state whose axis is rotated by $\pi/2$ (with respect to the axis of the given oblate state). Since the family of critical points corresponding to $r_2(\tau)$ is isolated when $\tau \in (0, \tau_c)$ and $\tau \in (\tau_c, \tau^*)$, employing proposition 1 once again, we conclude that it is unstable for all $\tau \in (0, \tau^*)$. When $\tau = \tau_c$ this branch 'collides' with the trivial solution, and its energy is greater than that of $\rho_1(s)$; thus it is unstable (again, we may use the energy comparison because at this temperature there exist only two nonequivalent critical states). The bifurcation at $\tau = \tau_c$ is transcritical; however, note that the states do not exchange stability: both of them become unstable after collision. Summarizing all of the above we may formulate the following theorem.

Theorem 4. *When $\tau > \tau^* \approx 0.149$ the only critical point of the free energy functional (1) with Maier–Saupe interaction potential is the uniform density $\bar{\rho} \equiv 1/4\pi$, which is the global minimizer. It remains the global minimizer when $\tau > \tau_* \approx 0.148$ and a local minimizer when $\tau \in (\tau_c, \tau_*]$; it loses stability when $\tau \leqslant \tau_c$. For $\tau < \tau^*$ there exist exactly two families of rotation-equivalent nontrivial critical points described by theorem 1, corresponding to the two branches of the function $r(\tau)$ (these branches merge at $\tau = \tau^*$). One of these families consists of stable (local non-isolated minimizers) prolate states which also become global (non-isolated) minimizers when $\tau \in (0, \tau_*)$. The other family consists of unstable prolate states when $\tau \in (\tau_c, \tau^*]$ and unstable oblate states when $\tau \in (0, \tau_c)$.*

As in the case of dipolar interaction we also present the leading-order asymptotic expansions of the order parameter r as a function of τ; the corresponding graphs are displayed in figure 2.

$$\begin{aligned} r_1 &= -\frac{1}{3\tau} + \mathcal{O}(1), \quad r_2(\tau) = \frac{1}{6\tau} + \mathcal{O}(1), \qquad \tau \downarrow 0; \\ r_2 &= \frac{105}{4}(\tau_c - \tau) + \mathcal{O}(\tau_c - \tau)^2, \qquad \tau \to \tau_c. \end{aligned} \tag{37}$$

4. Discussion

We obtained explicit expressions for all critical points of the Onsager free energy functional (1) with dipolar (2) and Maier–Saupe (3) interaction potentials. The first step in our approach is an observation that the thermodynamic potential $\Phi(s)$ belongs to the same eigenspace of the Laplace–Beltrami operator as the interaction potential $U(s, s')$. It turns out that for the dipolar interaction, any function from the corresponding eigenspace is a solution of the Euler–Lagrange equation (9) for some value of the temperature τ. Thus this case is completely analogous to the reduced model on a circle [9]. However, this is not true for the Maier–Saupe interaction: only axially symmetric functions from the respective eigenspace are solutions. We proved this fact via careful analysis of the Euler–Lagrange equation using semi-explicit representation of the partition integral by means of Bessel functions. Although our proof is not very technical, we believe that a simpler proof, based exclusively on the symmetry properties of the model, is possible; however we were not able to find it. Following classification of critical points we analysed their stability and studied bifurcations which occur as the temperature is varied.

On a final note let us mention that the calculation for the dipolar interaction potential may be straightforwardly generalized to a sphere in a Euclidean space of an arbitrary dimension d. In this case the trivial solution is the unique critical point when $\tau \geqslant 1/d$. When $\tau < 1/d$ it loses stability as a result of a pitchfork bifurcation, and a family of rotation-equivalent critical points (global non-isolated minimizers) appears. The latter are given by

$$\rho(s) = \mathcal{Z}^{-1}\, \mathrm{e}^{-r\cos\theta}, \qquad \mathcal{Z} = 2\pi \left[\frac{2\pi}{r}\right]^{d/2-1} \mathrm{I}_{d/2-1}(r), \qquad \tau = \frac{1}{r}\frac{\mathrm{d}}{\mathrm{d}r} \ln \mathcal{Z}. \tag{38}$$

Here θ is the polar angle with respect to an arbitrarily chosen polar axis, and $r > 0$ is determined uniquely for an arbitrary $\tau \in (0, 1/d)$. No other critical points exist.

Acknowledgments

The authors are grateful to the referees for valuable suggestions and references to the earlier articles on similar topics. Additional thanks are due to A Yu Grosberg for informative discussions and reference [14]. VS acknowledges support by NSF grant DMS-0405343.

Appendix A. Axial symmetry of thermodynamic potential for the Maier–Saupe interaction

In this section we prove the main lemma which implies the axial symmetry of solutions for the model with the Maier–Saupe interaction potential. Consider the following equations ($\tau > 0$ is a parameter):

$$\mathcal{Z}\lambda_i = \tau \frac{\partial \mathcal{Z}}{\partial \lambda_i}, \qquad \mathcal{Z} := \int_{|\boldsymbol{x}|=1} \exp\left\{\frac{1}{\tau}\sum_{i=1}^{3}\lambda_i x_i^2\right\} \mathrm{d}s(\boldsymbol{x}) \tag{A1}$$

Lemma 1. *Let a set of real numbers, $\{\lambda_1, \lambda_2, \lambda_3\}$, be a solution of (A1). Then necessarily: (i) $0 < \lambda_1, \lambda_2, \lambda_3 < 1$; (ii) $\lambda_1 + \lambda_2 + \lambda_3 = 1$; (iii) $\lambda_i = \lambda_j$ for some $i \neq j$.*

Proof. Conditions (i) and (ii) follow directly from (A1). Thus it only remains to prove (iii). Without loss of generality, let us label the eigenvalues so that

$$\lambda_1 \leqslant \lambda_2 < \lambda_3, \qquad \lambda_1 < \tfrac{1}{3} < \lambda_3. \tag{A2}$$

Indeed, if $\lambda_2 = \lambda_3$, (iii) already holds; the second inequality is then implied by (ii). We will prove that under stated conditions, a solution of (A1) may only occur if $\lambda_1 = \lambda_2$.

Our method is to construct a function which turns to zero whenever (A1) is satisfied. We then show that, in a suitable range of parameters, this function has at most one zero, which corresponds to $\lambda_1 = \lambda_2$. (Note that $\lambda_1 = \lambda_2 = (1 - \lambda_3)/2$ is a solution which may be verified either by a direct calculation, or using equivalence of (A1) and the Euler–Lagrange equation (33), for which this combination of eigenvalues produces an axially-symmetric solution.)

Let us make a change of variables in the λ-space, introducing parameters a, b and c:

$$\begin{gathered} a := \frac{\lambda_2 + \lambda_3}{6\tau} - \frac{\lambda_1}{3\tau}, \qquad b := \frac{\lambda_3 - \lambda_2}{2\tau}, \qquad c := \frac{\lambda_1 + \lambda_2 + \lambda_3}{3\tau}; \\ \lambda_1 = \tau(c - 2a), \qquad \lambda_2 = \tau(c + a - b), \qquad \lambda_3 = \tau(c + a + b). \end{gathered} \tag{A3}$$

Our convention regarding the labelling of λ_i translates into $a, b > 0$. This will be assumed from now on. We may write (A1) in terms of the new variables a, b, c as

$$6\tau\mathcal{Z}a = \frac{\partial \mathcal{Z}}{\partial a}, \qquad 2\tau\mathcal{Z}b = \frac{\partial \mathcal{Z}}{\partial b}, \qquad 3\tau\mathcal{Z}c = \frac{\partial \mathcal{Z}}{\partial c}. \tag{A4}$$

We may also derive the partial derivatives of $\mathcal{Z}$ from its explicit representation: introducing spherical coordinates ($\varphi \in [0, 2\pi)$, $\theta \in [0, \pi]$) such that

$$x_1 = \cos\theta, \qquad x_2 = \sin\theta\sin\varphi, \qquad x_3 = \sin\theta\cos\varphi, \tag{A5}$$

we obtain

$$\frac{1}{\tau}\sum_{i=1}^{3}\lambda_i x_i^2 = c - 2a + \sin^2\theta[3a + b\cos 2\varphi]. \tag{A6}$$

Using this relation in (A1) and integrating over the φ-variable (employing Sommerfeld's representation (A11) of Bessel functions, see [12]) we get

$$\mathcal{Z} = 2\pi \mathrm{e}^{c-2a} \int_0^\pi \mathrm{e}^{3a\sin^2\theta} \mathrm{I}_0(b\sin^2\theta)\sin\theta\,\mathrm{d}\theta = 2\pi\,\mathrm{e}^{c-2a} \int_0^1 \frac{\mathrm{e}^{3a\gamma}\mathrm{I}_0(b\gamma)}{\sqrt{1-\gamma}}\,\mathrm{d}\gamma. \tag{A7}$$

From here we deduce,

$$\begin{aligned} \frac{\partial \mathcal{Z}}{\partial a} &= 6\pi\,\mathrm{e}^{c-2a} \int_0^1 \gamma \frac{\mathrm{e}^{3a\gamma}\,\mathrm{I}_0(b\gamma)}{\sqrt{1-\gamma}}\,\mathrm{d}\gamma - 2\mathcal{Z}, \\ \frac{\partial \mathcal{Z}}{\partial b} &= 2\pi\,\mathrm{e}^{c-2a} \int_0^1 \gamma \frac{\mathrm{e}^{3a\gamma}\mathrm{I}_1(b\gamma)}{\sqrt{1-\gamma}}\,\mathrm{d}\gamma, \\ \frac{\partial \mathcal{Z}}{\partial c} &= \mathcal{Z}. \end{aligned} \tag{A8}$$

Comparing with (A4) we obtain the following equalities (expressions for $3\tau\mathcal{Z}\mathrm{e}^{2a-c}/\pi$):

$$\frac{1}{a}\int_0^1 (3\gamma-2)\frac{\mathrm{e}^{3a\gamma}\mathrm{I}_0(b\gamma)}{\sqrt{1-\gamma}}\,\mathrm{d}\gamma = \frac{3}{b}\int_0^1 \gamma\frac{\mathrm{e}^{3a\gamma}\mathrm{I}_1(b\gamma)}{\sqrt{1-\gamma}}\,\mathrm{d}\gamma = \frac{2}{c}\int_0^1 \gamma\frac{\mathrm{e}^{3a\gamma}\mathrm{I}_0(b\gamma)}{\sqrt{1-\gamma}}\,\mathrm{d}\gamma. \tag{A9}$$

The first equality implies that whenever (A1) is satisfied, the function

$$\mathcal{J}(a,b) := \int_0^1 \frac{\mathrm{e}^{3a\gamma}}{\sqrt{1-\gamma}}\left[(3\gamma-2)\mathrm{I}_0(b\gamma) - \frac{3a\gamma}{b}\mathrm{I}_1(b\gamma)\right]\mathrm{d}\gamma, \tag{A10}$$

turns to zero. Using proposition 2 we know that for a given $a > 0$ there exists at most one zero of $\mathcal{J}(a,b)$ when b is varied over $(0,\infty)$. Then this zero necessarily occurs at $b = 3a$, or equivalently, $\lambda_1 = \lambda_2$ (since we know that such a set of λs produces a solution). One may also verify that $\mathcal{J}(a,3a) = 0$ computing the integral explicitly (see [12]). This completes the proof. □

Finally we prove the propositions employed above. Let us first state and prove a few auxiliary inequalities. Their proof uses the following standard relations (see, e.g. [12])

$$\mathrm{I}_n(z) = \frac{1}{\pi}\int_0^\pi \mathrm{e}^{z\cos\phi}\cos n\phi\,\mathrm{d}\phi \qquad \text{(Sommerfeld's representation, } n\in\mathbb{Z}\text{)}; \tag{A11}$$

$$\frac{\nu\mathrm{I}_\nu(z)}{z} = \mathrm{I}_{\nu-1}(z) - \frac{\mathrm{d}\mathrm{I}_\nu(z)}{\mathrm{d}z} = \mathrm{I}_{\nu+1}(z) + \frac{\mathrm{d}\mathrm{I}_\nu(z)}{\mathrm{d}z} = \frac{\mathrm{I}_{\nu-1}(z)-\mathrm{I}_{\nu+1}(z)}{2}. \tag{A12}$$

Lemma 2. *Assume $z \geqslant 0$, then (equalities are achieved if and only if $z = 0$)*

$$\mathrm{I}_0(z) > \mathrm{I}_1(z); \tag{A13}$$

$$\mathrm{I}_1^2(z) \geqslant \mathrm{I}_0(z)\mathrm{I}_2(z); \tag{A14}$$

$$2\mathrm{I}_0(z)\mathrm{I}_1(z) \geqslant z[\mathrm{I}_0^2(z) - \mathrm{I}_1^2(z)]; \tag{A15}$$

$$\frac{\mathrm{d}}{\mathrm{d}z}\left[z\frac{\mathrm{I}_1(z)}{\mathrm{I}_0(z)}\right] \geqslant 0. \tag{A16}$$

Proof. (A13) follows directly from (A11). To obtain (A14) use (A12) and derive

$$\frac{\mathrm{d}}{\mathrm{d}z}[\mathrm{I}_1^2(z) - \mathrm{I}_0(z)\mathrm{I}_2(z)] = \frac{2\mathrm{I}_0(z)\mathrm{I}_2(z)}{z} \geqslant 0. \tag{A17}$$

Setting $\nu = 1$ in (A12), multiplying by $\mathrm{I}_0(z)$ and using (A14) we obtain (A15). (A16) is verified by straightforward computation using (A12) and (A13). □

Proposition 2. *Fix $a > 0$. The function, $\mathcal{J}(a, b)$, defined by (A10) has at most one zero when $b \in (0, \infty)$.*

Proof. We prove this demonstrating that $\partial\mathcal{J}(a, b)/\partial b > 0$, whenever $\mathcal{J}(a, b) = 0$, $b > 0$. After a few manipulations with Bessel functions, we obtain

$$\frac{\partial\mathcal{J}(a, b)}{\partial b} = \int_0^1 \frac{\gamma e^{3a\gamma}}{\sqrt{1-\gamma}}\left[(3\gamma - 2)\mathrm{I}_1(b\gamma) - \frac{3a\gamma}{b}\mathrm{I}_2(b\gamma)\right]\mathrm{d}\gamma. \tag{A18}$$

Using (A14) we get

$$b\frac{\partial\mathcal{J}(a, b)}{\partial b} > \int_0^1 \frac{e^{3a\gamma}}{\sqrt{1-\gamma}}\left[(3\gamma - 2)\mathrm{I}_0(b\gamma) - \frac{3a\gamma}{b}\mathrm{I}_1(b\gamma)\right]\frac{\mathrm{I}_1(b\gamma)b\gamma}{\mathrm{I}_0(b\gamma)}\,\mathrm{d}\gamma. \tag{A19}$$

Using proposition 3 we see that the function

$$f(\gamma) := b(3\gamma - 2)\mathrm{I}_0(b\gamma) - 3a\gamma\mathrm{I}_1(b\gamma), \tag{A20}$$

has at most one zero, $\gamma = \gamma^*$, in the interval $0 \leqslant \gamma \leqslant 1$ (it has to have a zero if $\mathcal{J}(a, b) = 0$). Now let $\mathcal{J}(a, b) = 0$. From the definition (A10) we then obtain

$$\int_0^{\gamma^*} \frac{\gamma e^{3a\gamma}}{\sqrt{1-\gamma}} f(\gamma)\,\mathrm{d}\gamma = -\int_{\gamma^*}^1 \frac{\gamma e^{3a\gamma}}{\sqrt{1-\gamma}} f(\gamma)\,\mathrm{d}\gamma. \tag{A21}$$

Taking into account relation (A16) and the fact that $f(\gamma)$ is negative for $\gamma < \gamma^*$ and positive for $\gamma > \gamma^*$, we conclude that

$$\int_0^{\gamma^*} \frac{\gamma e^{3a\gamma}}{\sqrt{1-\gamma}} f(\gamma)\frac{\mathrm{I}_1(b\gamma)b\gamma}{\mathrm{I}_0(b\gamma)}\,\mathrm{d}\gamma > -\int_{\gamma^*}^1 \frac{\gamma e^{3a\gamma}}{\sqrt{1-\gamma}} f(\gamma)\frac{\mathrm{I}_1(b\gamma)b\gamma}{\mathrm{I}_0(b\gamma)}\,\mathrm{d}\gamma. \tag{A22}$$

(This follows if we note that the integral term on the left-hand side is multiplied by a positive function which is uniformly less than the respective multiplier on the right-hand side.) Collecting both terms on the left-hand side and comparing with (A19) we obtain

$$\frac{\partial\mathcal{J}(a, b)}{\partial b} > \frac{1}{b^2}\int_0^1 \frac{\gamma e^{3a\gamma}}{\sqrt{1-\gamma}} f(\gamma)\frac{\mathrm{I}_1(b\gamma)b\gamma}{\mathrm{I}_0(b\gamma)}\,\mathrm{d}\gamma > 0, \tag{A23}$$

which concludes the proof. □

Proposition 3. *Take any $a, b > 0$. The function $f(z) := b(3z - 2b)\mathrm{I}_0(z) - 3az\mathrm{I}_1(z)$ has at most one zero within $[0, b]$.*

Proof. It is sufficient to consider $2b/3 \leqslant z \leqslant b$, since $f(z)$ is strictly negative when $0 \leqslant z < 2b/3$. Let us introduce an auxiliary function $g(z) := f(z)/[z\mathrm{I}_1(z)]$. Observe that zeros of $f(z)$ and $g(z)$ coincide. We will prove that $g(z)$ is an increasing function when $z \in [2b/3, b]$ and thus has at most one zero within this interval. By direct computation

$$g'(z) = \frac{3b}{z}\frac{\mathrm{I}_0(z)}{\mathrm{I}_1(z)} + b(3z - 2b)\frac{\mathrm{I}_1^2(z) - \mathrm{I}_0^2(z)}{z\mathrm{I}_1^2(z)} > \frac{3b}{z}\frac{\mathrm{I}_0(z)}{\mathrm{I}_1(z)} - \frac{2b(3z - 2b)}{z^2}\frac{\mathrm{I}_0(z)}{\mathrm{I}_1(z)}. \tag{A24}$$

For the inequality we used $3z - 2b \geqslant 0$ and relation (A15). Rearranging the terms we obtain

$$g'(z) > \frac{b(4b - 3z)}{z^2}\frac{\mathrm{I}_0(z)}{\mathrm{I}_1(z)} > 0, \tag{A25}$$

where $z < b$ was used for the second inequality. Thus $g(z)$ is a strictly increasing function on $[2b/3, b]$ and consequently has at most one zero within this interval. Since $f(z)$ has no zeros in $[0, 2b/3)$ and the same zeros as $g(z)$ in $[2b/3, b]$, we conclude that $f(z)$ has at most one zero in $[0, b]$. □

Appendix B. Some properties of spherical harmonics and related functions

Let us summarize a few properties of spherical harmonics $y_{l,m}(s)$ that we employ in this work. In a spherical coordinate frame ($\varphi \in [0, 2\pi)$, $\theta \in [0, \pi]$) we may represent the functions $y_{l,m}(s)$ as

$$y_{l,m}(\varphi, \theta) := \left[\frac{2l+1}{4\pi}\frac{(l-|m|)!}{(l+|m|)!}\right]^{1/2} P_l^{|m|}(\cos\theta)\mathrm{e}^{\mathrm{i}m\varphi}, \qquad l = 0, 1, \ldots, m = -l, \ldots, l. \tag{B1}$$

The associated Legendre functions $P_l^m(z)$ (for positive integer m) are given by

$$P_l^m := (1-z^2)^{m/2}\frac{\mathrm{d}^m}{\mathrm{d}z^m}P_l(z), \tag{B2}$$

where $P_l(x)$ are the Legendre polynomials

$$P_l(z) := \frac{1}{2^l l!}\frac{\mathrm{d}^l}{\mathrm{d}z^l}(z^2-1)^l, \qquad l = 0, 1, \ldots. \tag{B3}$$

Note that harmonics $y_{l,m}(s)$ with positive index m are sometimes defined with $(-1)^m$ sign; we do not use this convention for notational simplicity, in this case $y^*_{l,m}(s) = y_{l,-m}(s)$.

The spherical harmonics are the eigenfunctions of the Laplace–Beltrami operator on $\mathbb{S}^2$:

$$\Delta := \frac{1}{\sin\theta}\frac{\partial}{\partial\theta}\sin\theta\frac{\partial}{\partial\theta} + \frac{1}{\sin^2\theta}\frac{\partial^2}{\partial\varphi^2}. \tag{B4}$$

Namely, we have

$$\Delta y_{l,m}(s) = -l(l+1)y_{l,m}(s). \tag{B5}$$

The lth eigenvalue is $2l+1$-degenerate and the corresponding eigenspace Λ_l, a subspace of $\mathbb{L}^2(\mathbb{S}^2)$, is spanned by $y_{l,m}(s)$, $m = -l, \ldots, l$. Harmonics with different indices are orthogonal; the normalizing coefficients in (B1) are chosen so that $y_{l,m}(s)$ comprise an orthonormal basis.

In our work we use harmonics of the orders $l = 1, 2$. For instructive purposes let us write them down explicitly:

$$\begin{aligned}
&y_{1,0}(\varphi,\theta) := \left[\frac{3}{4\pi}\right]^{1/2}\cos\theta, \qquad y_{1,\pm1}(\varphi,\theta) := \left[\frac{3}{8\pi}\right]^{1/2}\sin\theta\,\mathrm{e}^{\pm\mathrm{i}\varphi}\\
&y_{2,0}(\varphi,\theta) := \left[\frac{5}{16\pi}\right]^{1/2}(3\cos^2\theta - 1),\\
&y_{2,\pm1}(\varphi,\theta) := \left[\frac{15}{32\pi}\right]^{1/2}\sin 2\theta\,\mathrm{e}^{\pm\mathrm{i}\varphi}, \qquad y_{2,\pm2}(\varphi,\theta) := \left[\frac{15}{32\pi}\right]^{1/2}\sin^2\theta\,\mathrm{e}^{\pm2\mathrm{i}\varphi}.
\end{aligned} \tag{B6}$$

An essential property is the so-called addition theorem for spherical harmonics [12]. Consider two unit vectors $\boldsymbol{x}$ and $\boldsymbol{x}'$ in $\mathbb{R}^3$. Let s and s' denote respective points on the unit sphere with centre at the origin; then

$$P_l(\boldsymbol{x}\cdot\boldsymbol{x}') = \frac{4\pi}{2l+1}\sum_{m=-l}^{l} y_{l,m}(s)y'_{l,m}(s'). \tag{B7}$$

Finally, we prove a useful lemma regarding axially-symmetric functions on the sphere.

Lemma 3. *A function $\Psi \in \mathbb{L}^2(\mathbb{S}^2)$ is axially-symmetric (invariant with respect to rotations around some axis) if and only if it may be expanded in terms of the spherical harmonics with index $m = 0$:*

$$\Psi(s) = \sum_{l=0}^{\infty}\psi_l y_{l,0}(s). \tag{B8}$$

Proof. Let $\Psi(s)$ be axially symmetric. Choosing the axis of symmetry as the polar axis and expanding $\Psi(s)$ in terms of respective spherical harmonics we get that for any φ'

$$\sum_{l=0}^{\infty}\sum_{m=-l}^{l}\psi_{l,m}y_{l,m}(\varphi,\theta)=\Psi(\varphi,\theta)=\Psi(\varphi+\varphi',\theta)=\sum_{l=0}^{\infty}\sum_{m=-l}^{l}\mathrm{e}^{\mathrm{i}m\varphi'}\psi_{l,m}y_{l,m}(\varphi,\theta). \tag{B9}$$

Since $\{y_{l,m}(\varphi,\theta)\}$ is a basis in $\mathbb{L}^2$, $\psi_{l,m}=0$ for any $m\neq 0$. The converse statement is obvious: $\Psi(s)$ is invariant with respect to all rotations around the polar axis. □

References

[1] Bhandar A S and Wiest J M 2003 Mesoscale constitutive modeling of magnetic dispersions *J. Colloid Interface Sci.* **257** 371–82

[2] Bhave A V, Menon R K, Armstrong R C and Brown R A 1993 A constitutive equation for liquid–crystalline polymer solutions *J. Rheol.* **37** 413–41

[3] Constantin P, Kevrekidis I G and Titi E S 2004 Asymptotic states of a Smoluchowski equation *Arch. Rat. Mech. Anal.* **174** 365–84

[4] Constantin P, Kevrekidis I G and Titi E S 2004 Remarks on a Smoluchowski equation *Discrete Cont. Dyn. Syst.* **11** 101–12

[5] Constantin P and Vukadinovic J 2005 Note on the number of steady states for a 2D Smoluchowski equation *Nonlinearity* **18** 441–3

[6] de Gennes P G and Prost J 1993 *The Physics of Liquid Crystals* (Oxford: Oxford University Press)

[7] Doi M 1981 Molecular dynamics and rheological properties of concentrated solutions of rodlike polymers in isotropic and liquid crystalline phases *J. Polym. Sci. Polym. Phys. Edn* **19** 229–43

[8] Doi M and Edwards S F 1986 *The Theory of Polymer Dynamics* (Oxford: Oxford University Press)

[9] Fatkullin I and Slastikov V 2005 A note on the Onsager model of nematic phase transitions *Commun. Math. Sci.* **3** 21–6

[10] Forest M G, Wang Q and Zhou R 2004 The weak shear kinetic phase diagram for nematic polymers *Rheol. Acta* **43** 17–37

[11] Freiser M J 1970 Ordered states of a nematic liquid *Phys. Rev. Lett.* **24** 1041–3

[12] Gradshteyn I S and Ryzhik I M 1965 *Table of Integrals, Series, and Products* (New York: Academic)

[13] Grosberg A Yu and Khokhlov A R 1994 *Statistical Physics of Macromolecules* (New York: AIP Press)

[14] Kayser R F Jr and Raveché H J 1978 Bifurcation in Onsager's model of isotropic–nematic transition *Phys. Rev.* A **17** 2067–72

[15] Krasnosel'skii M A 1964 *Topological Methods in the Theory of Nonlinear Integral Equations* (Oxford: Pergamon)

[16] Kröger M 2004 Simple models for complex nonequilibrium fluids *Phys. Rep.* **390** 453–551

[17] Larson R G and Ottinger H C 1991 Effect of molecular elasitcity on out-of-plane orientations in shearing flows of liquid-crystalline polymers *Macromolecules* **24** 6270–82

[18] Luo C, Zhang H and Zhang P 2005 The structure of equilibrium solutions of the one-dimensional Doi equation *Nonlinearity* **18** 379–89

[19] Maier W and Saupe A 1958 Eine einfache molekulare Theorie des nematischen kristallinflüssigen Zustandes *Z. Naturf.* a **13** 564

[20] Onsager L 1949 The effects of shape on the interaction of colloidal particles *Ann. NY Acad. Sci.* **51** 627–59

[21] Wang Q 1997 Biaxial steady states and their stability in shear flows of liquid crystal polymers *J. Rheol.* **41** 943–70

[22] Zeidler E 1984 *Nonlinear Functional Analysis and its Applications III: Variational Methods and Optimization* (Berlin: Springer)